

Mass relations of mirror nuclei for both bound and unbound systems

Y. Y. Zong,¹ C. Ma,¹ M. Q. Lin,¹ and Y. M. Zhao^{1,2,*}

¹*Shanghai Key Laboratory of Particle Physics and Cosmology, School of Physics and Astronomy,
Shanghai Jiao Tong University, Shanghai 200240, China*

²*Collaborative Innovation Center of IFSA (CICIFSA), Shanghai Jiao Tong University, Shanghai 200240, China*



(Received 8 May 2021; revised 11 February 2022; accepted 3 March 2022; published 21 March 2022)

In this paper we study nuclear masses of proton-rich systems close to (both inside and outside) the proton drip line, in terms of mass relations for mirror nuclei. We show that mass relations of mirror nuclei are remarkably accurate for *all* nuclei (including very light nuclei) within the proton drip line, with root-mean-square deviations (RMSD) between 70–147 keV. A very simple formula is proposed to extend the mass relations to systems beyond the proton drip line, with the RMSD value of 183 keV (or 164 keV if the $^{11}\text{O} - ^{11}\text{Li}$ mirror partners are excluded). Based on these mass relations, we predict 162 mass excesses of proton-rich systems (136 systems outside and 26 systems inside the proton drip line) close to the proton drip line, and tabulate these results in the Supplemental Material of this paper.

DOI: [10.1103/PhysRevC.105.034321](https://doi.org/10.1103/PhysRevC.105.034321)

Nuclear mass M , neutron separation energy S_n , and proton separation energy S_p , are not only fundamental quantities of atomic nuclei, but also are important inputs in astrophysics and some other branches of science. In past decades many efforts have been devoted to predicting nuclear masses and nucleon separation energies [1,2]. Here, we mention a few “global” models, such as the Dufflo-Zuker model [3], the finite range droplet model (FRDM) [4,5], the Skyrme Hartree-Fock-Bogoliubov theory [6], and Weizsäcker-Skyrme (WS) model [7,8]. There are also local mass relations, such as the Audi-Wapstra extrapolation method [9–11], the Garvey-Kelson mass relations [12,13], and mass relations based on neutron-proton interactions [14,15]. Between global mass models and local mass relations, there is another approach which is based on isospin symmetry of the nuclear force, called mass relations of mirror nuclei [16–21]. In recent years, such relations have been demonstrated to be remarkably accurate. Yet these relations have been applied to nuclei with a constraint that mass number A is between 20 and 90, and within the proton drip line.

In this paper we show that mass relations of mirror nuclei are actually robust for $A \leq 20$, if we restrict ourselves to proton-rich nuclei within the proton drip line. With simple corrections, we further extend these relations to nuclear systems beyond the proton drip line; these relations are found to be also remarkably accurate.

Let us begin our discussion by revisiting mass relations of mirror nuclei. We use $M(N, Z)$ to denote the mass of nucleus with N neutrons and Z protons. According to the Weizsäcker

mass formula, $M(N, Z)$ is written as follows:

$$\begin{aligned} M(N, Z) &\equiv NM_n + ZM_p - B(N, Z) \\ &= NM_n + ZM_p - a_v A + a_s A^{2/3} + E_c \\ &\quad + a_a (N - Z)^2 A^{-1} - \delta_{\text{pair}}, \end{aligned} \quad (1)$$

where $A = N + Z$ is the mass number, M_n and M_p represent masses of a free neutron and a free proton, respectively; the terms with parameters a_v , a_s , a_a are called the volume, surface, and symmetry terms, respectively, and δ_{pair} is called the pairing term. E_c is called the Coulomb energy term, which is usually assumed to take the value of a uniformly charged sphere with Z protons,

$$E_c = \frac{3}{5} \frac{1}{4\pi\epsilon_0} \frac{Z^2 e^2}{A^{1/3} r_0} = a_c^{(0)} \frac{Z^2 e^2}{A^{1/3}}, \quad (2)$$

where $r_0 = 1.2$ fm is adopted. The value of $a_c^{(0)}$,

$$a_c^{(0)} = \frac{3}{5} \frac{e^2}{4\pi\epsilon_0 r_0} \simeq 0.720 \text{ MeV}.$$

Instead of N and Z , as in previous papers, we use $M(K - k, K)$ and $M(K, K - k)$ to represent the masses of mirror nuclei, with $M(K - k, K)$ the proton-rich and $M(K, K - k)$ the neutron-rich, respectively. From Eqs. (1)–(2), one has

$$\begin{aligned} \Delta_m(K - k, K) &\equiv M(K - k, K) - M(K, K - k) \\ &= a_c^{(0)} k A^{2/3} - k \Delta E_{\text{np}}^{(0)}, \end{aligned} \quad (3)$$

where $\Delta E_{\text{np}}^{(0)}$ represents the mass difference of a proton and a neutron for atomic masses,

$$\Delta E_{\text{np}}^{(0)} = M_n - M_p - m_e = 0.782 \text{ MeV}.$$

*Corresponding author: ymzhao@sjtu.edu.cn

TABLE I. The RMSD (in keV) of Eqs. (5), (11)–(12), (15), and (16) and the parameters a' , α , and β (in units of keV) optimized based on AME2020 database. It is noted that the resultant RMSD and the values of these three parameters are very robust, namely, one obtains almost the same values if one adopts the AME2012 or AME2016 database.

	RMSD	a'	α	β
Δ_m	147	-20 ± 2	67 ± 24	1276 ± 329
Δ_n, Δ_p	96	-16 ± 2	105 ± 24	1473 ± 150
S_p	96	-18 ± 3	70 ± 31	1500 ± 175
S_{2p}	151	-19 ± 3	67 ± 28	–

A more sophisticated Coulomb energy of atomic nuclei has been well known [22,23] as follows:

$$E_c = E_c^d + E_c^e + E_c^s$$

$$= a_c \frac{Z^2}{A^{1/3}} - \frac{5}{4} \left(\frac{3}{2\pi} \right)^{2/3} a_c \frac{Z^{4/3}}{A^{1/3}} - a_c \frac{Z}{A^{1/3}}, \quad (4)$$

where E_c^d , E_c^e , E_c^s are called the direct, the exchange and the self-energy terms, respectively. It has also been well known that E_c exhibits an odd-even staggering, which is a reflection of the short-range attractive pairing correlation between protons [22–24]. With such considerations, Eq. (3) is improved, and takes the following form:

$$\Delta_m(K-k, K)$$

$$= a_c k \delta_c^m - k \Delta E_{np} + \frac{1 - (-)^k}{2} (-)^K \frac{\beta}{A}, \quad (5)$$

where the last term represents an empirical odd-even staggering in Coulomb energy discussed in Ref. [20], and here this term is improved by introducing a mass-number A dependence, and

$$\delta_c^m = A^{2/3} - 0.808 - A^{-1/3}.$$

In this paper, we treat both a_c and ΔE_{np} as adjustable parameters,

$$a_c = a_c^{(0)} + a' = 0.720 + a' \text{ (MeV)}, \quad (6)$$

$$\Delta E_{np} = \Delta E_{np}^{(0)} + \alpha = 0.782 + \alpha \text{ (MeV)}, \quad (7)$$

where a' and α are expected to be small values (below 100 keV). All parameters are obtained by a χ^2 fitting procedure, which are explained in Appendix A. In the first row (labeled by Δ_m) of Table I, we present the optimized values of a' , α , and β of Eq. (5) based on the AME2020 database, for the Δ_m relation of Eq. (5).

The empirical neutron-proton interaction between the last neutron and last proton for nucleus with N neutrons and Z protons is defined by

$$V_{np}(N, Z) = -M(N, Z) - M(N-1, Z-1)$$

$$+ M(N, Z-1) + M(N-1, Z).$$

We denote the difference of the V_{np} of two mirror nuclei with $(N, Z) = (K-k, K)$ and $(N, Z) = (K, K-k)$ by $\Delta V_{np}(K-k, K) = V_{np}(K-k, K) - V_{np}(K, K-k)$. If the

isospin symmetry is exact, one has the simple ΔV_{np} relation as

$$\Delta V_{np} = 0. \quad (8)$$

In Refs. [18,19], differences of one-nucleon separation energies for mirror nuclei were introduced and examined. Let us define Δ_n and Δ_p ,

$$\Delta_n(K-k, K)$$

$$\equiv [M(K-k-1, K) - M(K-k, K)]$$

$$- [M(K, K-k-1) - M(K, K-k)]$$

$$= S_n(K-k, K) - S_p(K, K-k) - \Delta E_{np}^{(0)}, \quad (9)$$

$$\Delta_p(K-k, K)$$

$$\equiv [M(K-k, K-1) - M(K-k, K)]$$

$$- [M(K-1, K-k) - M(K, K-k)]$$

$$= S_p(K-k, K) - S_n(K, K-k) + \Delta E_{np}^{(0)}. \quad (10)$$

By using Eq. (5), we obtain

$$\Delta_n(K-k, K)$$

$$= (a_c^{(0)} + a') \delta_c^n - (\Delta E_{np}^{(0)} + \alpha) + (-)^P \frac{\beta}{A}, \quad (11)$$

$$\Delta_p(K-k, K)$$

$$= (a_c^{(0)} + a') \delta_c^p + (\Delta E_{np}^{(0)} + \alpha) - (-)^P \frac{\beta}{A}, \quad (12)$$

where the left-hand sides of the above two formulas are extracted from experimental data by using their definitions in Eqs. (9)–(10), and the neutron-proton mass ΔE_{np} and Coulomb energy coefficient a_c are treated as adjustable parameters, as defined in Eqs. (6)–(7). Here, P is the parity of the neutron number $K-k$ (proton number K) for the quantity Δ_n (Δ_p); and

$$\delta_c^n = (k+1)(A-2)(A-1)^{-1/3}$$

$$- k(A-1)A^{-1/3} - 0.808, \quad (13)$$

$$\delta_c^p = (k-1)(A-2)(A-1)^{-1/3}$$

$$- k(A-1)A^{-1/3} + 0.808. \quad (14)$$

In the second row of Table I we present the optimized parameters a' , α , and β in Eqs. (11)–(12) by using the AME2020 database. We note that the value of a_c , which was discriminated by their parity of proton and neutron numbers in Ref. [19], is now unified by introducing a simple mass dependence adopted in the pairing term of Eq. (5).

Figure 1 summarizes the deviation of Δ_m , Δ_n , Δ_p , and ΔV_{np} calculated by using Eqs. (5), (11), (12), and (8), respectively, from those extracted from the AME2020 database [25], for nuclei within the proton drip line. The root mean square deviation (RMSD) values of these results are in general very small (147, 90, 96, 70 keV, respectively); and those for $A \leq 20$ are 144, 112, 99, 141 keV, respectively. Therefore, mass relations of Eqs. (5), (8), and (11)–(12), are actually well applicable to all these nuclei within the proton drip line, including nuclei with a very small number of mass number

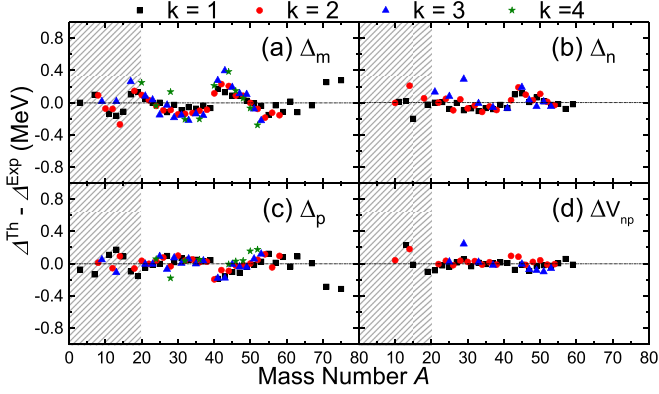


FIG. 1. Deviations (in unit of MeV) of theoretical Δ_m , Δ_n , Δ_p , and Δ_{np} from those extracted based on the AME2020 database [25], for nuclei within the proton drip line. The squares in black, circles in red, up triangles in blue, stars in olive corresponds to $k = 1-4$. The RMSD values of (a)–(d) are 147, 89, 96, 70 keV, respectively.

A. There have been many studies of masses for proton-rich light and medium nuclei by various models; yet there has been few efforts to construct simple and accurate mass formulas for nuclei in this region hitherto. It is also interesting and worthy to note that, empirically, candidates which have proton-halo ground states, e.g., one-proton-halo nuclei ${}^8\text{B}$ and ${}^{12}\text{N}$, or those for candidates of two-proton-halo nuclei ${}^{10}\text{C}$ and ${}^{17}\text{Ne}$ [26], do not exhibit sharp anomalies in these formulas.

Equations (11)–(12) are found to be very accurate in predictions. In Fig. 2 we demonstrate their predictive power by a few examples: Panels (a)–(d) plot those for which the deviations of masses in the AME2016 database from those in the AME2020 database are larger than 50 keV; panels (e)–(g) correspond to those which our predictions from those in the AME2020 database are the largest; and panels (h)–(l) correspond to those which are not accessible in the AME2016 database but accessible in the AME2020 database [25,27–30]. We note that the measurements of the three masses (for ${}^{28}\text{S}$, ${}^{71}\text{Kr}$, ${}^{75}\text{Sr}$) are warranted, one of the reasons is that the experimental uncertainties of these nuclei are large, and the other reason is that the RMSD would be 85 keV, which is sizably smaller than that in Table I (96 keV), if the values of these three nuclei in the AME2020 database were replaced by our predicted results. For this reason, we present our predicted mass excesses for these three nuclei, they are 4241(71) keV for ${}^{28}\text{S}$, $-46090(93)$ keV for ${}^{71}\text{Kr}$ and $-46362(93)$ keV for ${}^{75}\text{Sr}$, respectively (also see the Supplemental Material of Ref. [19]). As comparison, we list their mass excesses in the AME2020 database: 4070(160) keV for ${}^{28}\text{S}$, $-46330(130)$ keV for ${}^{71}\text{Kr}$, and $-46620(220)$ keV for ${}^{75}\text{Sr}$.

In Refs. [18,19], the predictions are made for neutron number N between 10 and 44. Because there are no experimental data of mass excesses $M(K, K-1)$ for $K = 45-50$, extrapolations of mass excesses by using Eqs. (11)–(12) are not possible for those with $Z > 44$. In order to evaluate masses of those nuclei by using Eqs. (11)–(12), one has to resort to predicted values of $M(K, K-1)$ with $K = 45-50$. In the AME2020 database [25], such mass excesses are predicted by extrapolations, and we adopt them as inputs of our predictions.

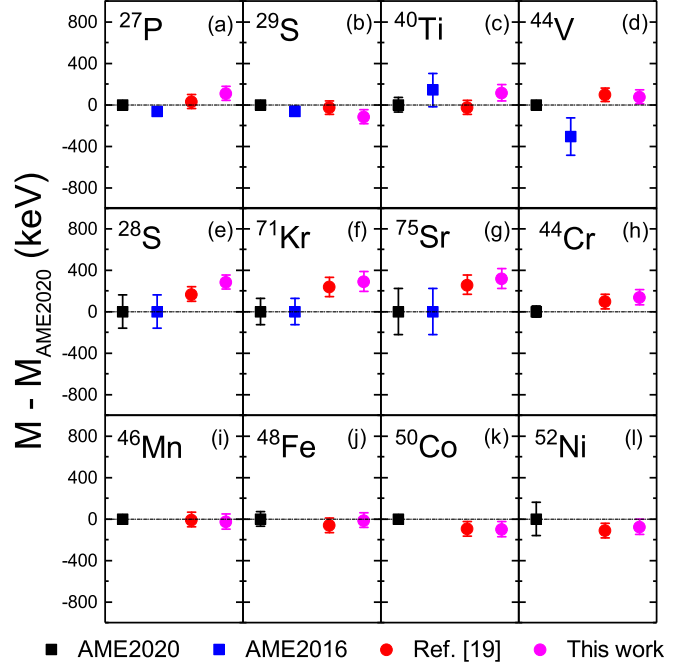


FIG. 2. Our predicted atomic masses in Ref. [19] and in this work, with respect to those in the AME2020 database. (a)–(d) correspond to cases for which the differences of nuclear masses in the AME2016 and those in the AME2020 database [25] are larger than 50 keV; (e)–(g) correspond to those our predicted results deviate from those in the AME2020 database larger than 150 keV; and (h)–(l) correspond to those inaccessible in the AME2016 database but accessible in the AME2020 database.

We note without details that, for these nuclei, the approach of δV_{1n-1p} [14] present predicted results which consistent with those in the AME2020 database within the theoretical uncertainties.

As one of the purposes in this paper is to discuss the masses of systems beyond the proton drip line, defined by either one-proton separation energy S_p to be negative or two-proton separation energy S_{2p} to be negative, we predict S_p and S_{2p} in cases that they are not accessible or not measured very accurately. From Eqs. (10) and (12), one obtains

$$S_p(K-k, K) = S_n(K, K-k) + a_c \delta_c^p + \alpha - (-)^K \frac{\beta}{A}, \quad (15)$$

where $S_n(K, K-k)$ is taken from experimental data, and $S_p(K-k, K)$ is our predicted value of one-proton separation energy of a nucleus with proton number K and neutron number $K-k$. Similarly, We define Δ_{2p} as

$$\begin{aligned} \Delta_{2p}(K-k, K) &\equiv [M(K-k, K-2) - M(K-k, K)] \\ &\quad - [M(K-2, K-k) - M(K, K-k)] \\ &= S_{2p}(K-k, K) - S_{2n}(K, K-k) + 2\Delta E_{np}^{(0)}. \end{aligned}$$

We obtain

$$S_{2p}(K-k, K) = S_{2n}(K, K-k) + a_c \delta_c^{2p} + 2\alpha, \quad (16)$$

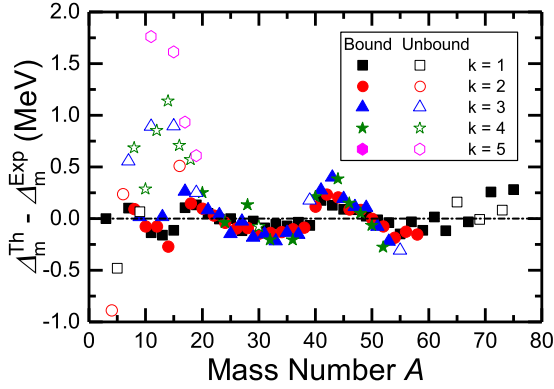


FIG. 3. Deviations of Δ_m mass relation for proton-rich nuclei both inside and beyond the proton drip line. The solid symbols correspond to cases for which the proton-rich nuclei are bound, while hollow symbols denote those for which the proton-rich systems are beyond the proton drip line. One sees the results deviates largely from zero if proton-rich partners of the mirror nuclei are beyond the proton drip line and when mass number is below 20.

where $S_{2n}(K, K - k)$ is taken from experimental data, and

$$\delta_c^{2p} = (k - 2)(A - 3)(A - 2)^{-1/3} - k(A - 1)A^{-1/3} + 1.616 \text{ MeV},$$

where 1.616 originated from 0.808 MeV (by two times) in Eq. (14). In Table I we present our optimized parameters of Eqs. (15) and (16), labeled by S_p and S_{2p} , respectively. Their RMSD values with respect to the AME2020 database are 96 keV and 151 keV, respectively.

Figure 3 plots the deviations of our predicted Δ_m from those extracted based on the AME2020 database [25], the same as Fig. 1(a) except that proton-rich systems beyond the proton drip line (denoted by hollow symbols) are considered. The results involved of systems beyond the proton drip line are easily seen to be “anomalous”, which deviate largely from zero; the further a nuclide from the drip line, the larger the deviation, in general. This behavior means that mass differences of mirror nuclei Δ_m extracted from experimental data, denoted by Δ_m^{Exp} , are smaller than those in cases that the proton-rich partners were within the proton drip line, namely, the results predicted by Eq. (5), denoted by Δ_m^{Th} . This deviation has two plausible origins, one is to take stronger attractive interaction among nucleons and the other is to reduce the Coulomb energy. Here, we take a simple scenario of smaller Coulomb energy, by assuming that the distribution of protons for a nucleus beyond the proton drip line is approximately represented by two parts, the inner part is a core with the “normal” density of protons, and the outer part is consisted of protons with a relatively smaller density. Following this scenario, we assume the nuclear charge density is given by

$$\rho = \begin{cases} \rho_1 + \rho_2, & 0 \leq r \leq R_1 \\ \rho_2, & R_1 \leq r \leq R_2 \end{cases}, \quad (17)$$

where $\rho_1 + \rho_2$ and R_1 are the normal nuclear charge density and corresponding radius of the sphere with this density, respectively; and ρ_2 and R_2 are the (smaller) nuclear charge

density out of the core part and corresponding radius. We assume the radius of the inner core $R_1 = r_0 A^{1/3}$, the same form of conventional distribution for nuclei close to the stability line. As we concentrate on the Coulomb energy, the distribution of neutrons does not contribute to the mass formulas in an explicit manner. We assume that neutrons for proton-rich systems outside the proton drip line stay essentially in the same orbits as protons in their neutron-rich mirror partners. We use k' to denote the number of protons from the core part which is assumed to be the nucleus right on the proton drip line. Thus the two densities are given by

$$\rho_1 = \frac{3(Z - k')}{4\pi R_1^3}, \quad \rho_2 = \frac{3k'}{4\pi R_2^3}. \quad (18)$$

The Coulomb energy for the unbound systems beyond the proton drip line is again given by three terms:

$$E_c = E_c^d + E_c^s + E_c^e, \quad (19)$$

where E_c^d , E_c^s , and E_c^e represent the direct term, exchange term, and self-energy term of the Coulomb energy, given as below. We define $\varepsilon = (R_2 - R_1)/R_2$, and obtain

$$E_c^d = \frac{a_c}{A^{1/3}} \left[(Z - k')^2 + \frac{k'(5Z - 3k')}{2}(1 - \varepsilon) - \frac{k'(Z - k')}{2}(1 - \varepsilon)^3 \right], \quad (20)$$

$$E_c^s = -\frac{a_c}{A^{1/3}}(Z - \varepsilon k'), \quad (21)$$

$$E_c^e = -\frac{5}{4} \left(\frac{3}{2\pi} \right)^{2/3} \frac{a_c}{A^{1/3}} [(Z - k')^{4/3} + (k')^{4/3}(1 - \varepsilon) + k'(Z - k')^{1/3}(1 - \varepsilon)^3]. \quad (22)$$

In the appendices of this paper, we present details of mathematical derivations for Eqs. (20)–(22). Instead of Eq. (4), we adopt Eq. (19) for the Coulomb energy, and have

$$\Delta'_m(K - k, K) = (a_c^{(0)} + a') \left(k\delta_c^m - k' \frac{\delta_c^{m'}}{A^{1/3}} \right) - k(\Delta E_{np}^{(0)} + \alpha), \quad (23)$$

where we use Δ'_m to denote the mass difference between the proton-rich system (beyond the proton drip line, with proton number K and neutron number $K - k$) and its neutron-rich mirror nucleus (with proton number $K - k$ and neutron number K), to discriminate the case in which both mirror nuclei are within the drip lines, and

$$\begin{aligned} \delta_c^m &= A^{2/3} - 0.808 - A^{-1/3}, \\ \delta_c^{m'} &= 2Z - k' - \varepsilon - \frac{5}{4k'} \left(\frac{3}{2\pi} \right)^{2/3} [Z^{4/3} - (Z - k')^{4/3}] \\ &\quad + (1 - \varepsilon) \left[\frac{5}{4} \left(\frac{3}{2\pi} \right)^{2/3} (k')^{1/3} - \frac{(5Z - 3k')}{2} \right] \\ &\quad + (Z - k')^{1/3} (1 - \varepsilon)^3 \left[\frac{5}{4} \left(\frac{3}{2\pi} \right)^{2/3} + \frac{(Z - k')^{2/3}}{2} \right]. \end{aligned}$$

One sees that in Eq. (23) that the value of k' , the number of protons outside the “core”, is important in our new mass

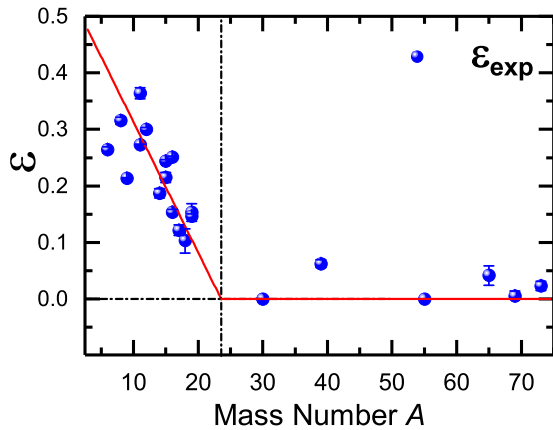


FIG. 4. The values of ε versus the mass number A . The solid spheres in blue are obtained by using recursive application of Eqs. (23)–(25), the solid straight line are theoretical values given by Eq. (25) with optimized parameters. The value of ε is sizable when $A \leq 23$, and is close to zero if $A > 23$.

formula. There is an ambiguity, however, concerning how to enumerate the number of k' : one enumerates this number either from the nucleus on the proton drip line but with the same neutron number, denoted by k_p here, or from the nucleus on the proton drip line but with the same proton number, denoted by k_n . The “effective” number of protons outside the nuclear “core” is expected to be in between these two numbers. Here, we assume a very simple form of k' in terms of k_p and k_n as follows.

$$k' = ck_n + (1 - c)k_p. \quad (24)$$

The parameter ε is empirically assumed to be proportional to mass number A ,

$$\varepsilon = aA + b. \quad (25)$$

The values of a , b , and c are optimized by using experimental data, and the resultant values are $a = -0.024 \pm 0.005$, $b = 0.553 \pm 0.070$, $c = 0.872 \pm 0.077$. A negative a is actually expected, as the Coulomb barriers are larger and thus differences between R_1 and R_2 become smaller for nuclei with larger mass A in general.

In Fig. 4 we plot “experimental” value of ε , denoted by ε_{exp} , versus the mass number A . The values of ε_{exp} are extracted by using recursive application of Eqs. (23)–(25), where $\Delta_m^{(\text{exp})}$ is determined from the experimental data, $a_c^{(0)} = 0.720$ MeV, and a' and α presented in the first row of Table I. From Fig. 4, one sees these ε_{exp} are far from zero for $A \leq 23$. For $A > 23$, $\varepsilon_{\text{exp}} \sim 0$, therefore we assume $\varepsilon = 0$ for $A > 23$, for simplicity. The resultant RMSD σ' of our calculated Δ'_m is 183 keV (or 164 keV if the ^{11}O system is excluded, as its mirror partner is the ^{11}Li , a typical neutron halo nucleus) from those extracted from the AME2020 database; this RMSD value is substantially smaller than that of Δ_m of Eq. (1) (which is 743 keV) for the same set of nuclei.

The remarkable accuracy of mass relations discussed in this paper is encouraging to predict masses of nuclei with $Z > N$ which are inaccessible experimentally. The nuclei that

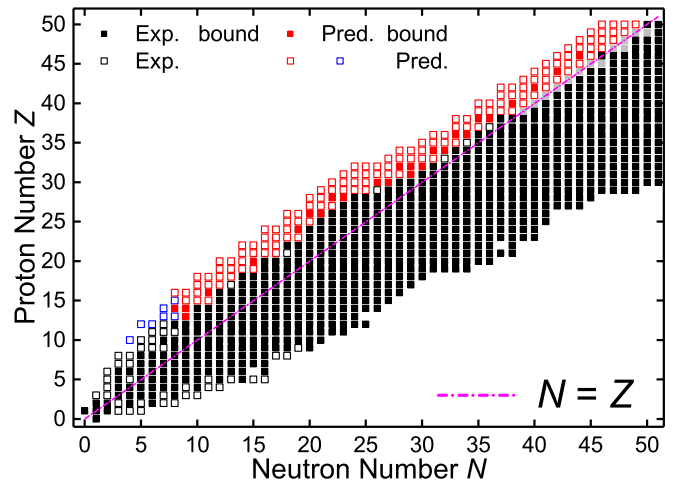


FIG. 5. The nuclide chart with our predicted mass excesses based on Δ_n , Δ_p , and Δ'_m relations. Solid symbols correspond to nuclei inside the proton drip line, and hollow symbols correspond to those beyond the proton drip line. Black squares corresponds to experimental data accessible in the AME2020 database, and gray squares were extrapolated in the AME2020 database. Red and blue squares are predicted by Eqs. (11)–(12) and Eq. (23), respectively. The magenta dashed line $N = Z$ is plotted to guide eyes.

we predict are summarized in Fig. 5, where the proton drip line is predicted by using Eqs. (15)–(16), solid squares in red correspond to nuclei within the proton drip line, and hollow squares correspond to proton-rich systems beyond the proton drip line. For the latter case, the mass excesses predicted by using Eq. (23) ($A \leq 23$) are denoted in blue, and those by using Eqs. (11)–(12) ($A > 23$) in red.

In total, among our predicted results, there are 26 cases inside and 136 cases outside the proton drip line. The experimental data of ^{28}S , ^{71}Kr , and ^{75}Sr are not adopted in our prediction due to their large experimental uncertainties. Our predicted results are tabulated in the Supplemental Material of this paper [31]. In Fig. 6, the deviations and theoretical uncertainties of our predicted results from extrapolated results in the AME2020 database are plotted versus mass number A . One sees that the deviations are relatively small (with the RMSD around or below 300 keV) for $k = 1-3$ and A between 70–100, and that our predicted results are in general smaller than those extrapolated in the AME2020 database.

To summarize, in this paper we revisit mass relations of mirror nuclei as a series of studies [18–21]. We are able to take *one unified set of parameters for odd and even values of proton number Z*. This improvement is realized by introducing an A dependence of the odd-even staggering term. We have shown that these relations are actually very accurate for nuclei from light-mass to medium-mass regions with very few exceptions, if one restricts to cases for which the proton-rich nuclei inside the proton drip line. Proton separation energies are investigated, with the RMSD values 96 keV for one-proton separation energies and 151 keV for two-proton separation energies.

Larger deviations arise in cases for which the proton-rich systems are beyond the proton drip line. Such deviations are

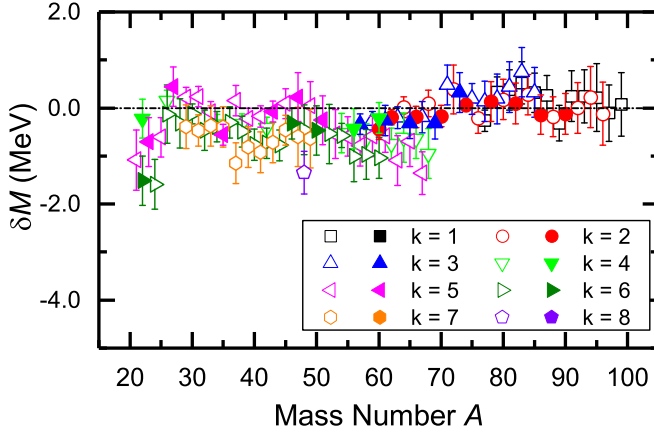


FIG. 6. Deviations (in units of MeV) of our predicted mass excess from those extrapolated in the AME2020 database [25]. The solid symbols correspond to nuclei inside the proton drip line, and the hollow symbols correspond to those beyond the proton drip line. Error bars are evaluated as the squared root of two uncertainties, theoretical uncertainty of this work and that in the AME2020 database. One sees that the deviations are relatively small for $k = 1-3$, but are sizable for $k = 4-8$ and $A \leq 60$.

suggested to be given by smaller Coulomb energy between protons outside the core part, marked by proton drip line. By assuming two densities for protons inside and outside the normal core part marked by the proton drip line, we propose a simple mass formula for those proton-rich systems beyond the proton drip line, with the RMSD 183 keV (or 164 keV if we exclude the O^{11} system for which its neutron-rich partner Li^{11} is a typical neutron-halo nucleus).

Based on our mass relations, we predict 162 proton-rich mass excesses around the proton drip line, including 26 systems inside and 136 systems outside the proton drip line. These predicted results are tabulated as a Supplemental Material of this paper [31], and compared with results extrapolated in the AME2020 database.

ACKNOWLEDGMENTS

We are very grateful to Prof. M. Wang for discussions and communications. We thank the National Natural Science Foundation of China (Grants No. 11975151 and 11961141003), and MOE Key Lab for Particle Physics, Astrophysics and Cosmology for financial support.

APPENDIX A: UNCERTAINTIES OF THE PARAMETER SET IN OUR MASS FORMULAS

In this Appendix we explain the uncertainties of our parameter set in Table I of this paper. Let us suppose we have a formula as follows:

$$y_i^{\text{th}} = \sum_{k=1}^M a_k X_k(x_i), \quad (\text{A1})$$

where $i = 1, 2, \dots, N$; $X_1(x), \dots, X_M(x)$ are functions of x , a_k ($k = 1, \dots, M$) are parameters of the above formula, and

M is the number of the parameters. The experimental values of y are denoted by $y_i \equiv y_i^{\text{exp}} \pm \sigma_i^{\text{exp}}$ ($i = 1, 2, \dots, N$).

In the χ^2 fitting process, the parameters a_k are obtained by minimizing the value of χ^2 which is defined by

$$\chi^2 = \sum_{i=1}^N \frac{(y_i^{\text{th}} - y_i^{\text{exp}})^2}{(\sigma_i^{\text{th}})^2 + (\sigma_i^{\text{exp}})^2} \quad (\text{A2})$$

with theoretical uncertainty σ_i^{th} determined iteratively by

$$(\sigma_i^{\text{th}})^2 = \frac{\sum_{i=1}^N w_i^2 [(y_i^{\text{th}} - y_i)^2 - (\sigma_i^{\text{exp}})^2]}{\sum_{i=1}^N w_i^2}, \quad (\text{A3})$$

where

$$w_i = \frac{1}{\sigma_i^2}. \quad (\text{A4})$$

We have

$$\chi^2 = \sum_{i=1}^N \frac{[\sum_{k=1}^M a_k X_k(x_i) - y_i]^2}{(\sigma_i^{\text{th}})^2 + (\sigma_i^{\text{exp}})^2}. \quad (\text{A5})$$

The above values of a_k are obtained with the following requirement:

$$\frac{\partial \chi^2}{\partial a_k} = 0, \quad (\text{A6})$$

and the uncertainties of a_k are given by

$$\sigma_{a_k} = \sqrt{\sum_{i=1}^N [(\sigma_i^{\text{th}})^2 + (\sigma_i^{\text{exp}})^2] \left(\frac{\partial a_k}{\partial y_i^{\text{th}}} \right)^2}. \quad (\text{A7})$$

The RMSD of the formula in Eq. (A1) is

$$\sigma = \sqrt{\sum_{i=1}^N \frac{(y_i^{\text{th}} - y_i)^2}{N}}. \quad (\text{A8})$$

APPENDIX B: DERIVATION OF $E_c^{d'}$ AND E_c^s

Suppose that there are k' protons outside the ‘‘core’’ part, with charge density ρ_2 , and the charge density of the core part is denoted by $\rho_1 + \rho_2$, as defined in Eq. (18). The strength of the electric field is as follows:

$$\vec{E} = \begin{cases} \frac{(\rho_1 + \rho_2)r}{3\epsilon_0} \vec{e}_r, & 0 \leq r \leq R_1 \\ \left(\frac{Z - k'}{4\pi\epsilon_0 r^2} + \frac{\rho_2 r}{3\epsilon_0} \right) \vec{e}_r, & R_1 \leq r \leq R_2. \\ \frac{Z}{4\pi\epsilon_0 r^2} \vec{e}_r, & r \geq R_2 \end{cases} \quad (\text{B1})$$

The total electric field energy of the system is given by an integral over the full three-dimensional space,

$$\int_0^\infty \frac{\epsilon_0}{2} \vec{E}^2 d^3\vec{r} = \frac{a_c}{A^{1/3}} \left[(Z - k')^2 - \frac{k'(Z - k')}{2} \left(\frac{R_1}{R_2} \right)^3 + \frac{k'(5Z - 3k')}{2} \frac{R_1}{R_2} \right]. \quad (\text{B2})$$

This is the direct term of Coulomb energy, denoted by $E_c^{d'}$. We denote $\varepsilon = (R_2 - R_1)/R_2$, and obtain

$$E_c^{d'} = \frac{a_c}{A^{1/3}} \left[(Z - k')^2 - \frac{k'(Z - k')}{2} (1 - \varepsilon)^3 + \frac{k'(5Z - 3k')}{2} (1 - \varepsilon) \right]. \quad (\text{B3})$$

This gives Eq. (20). The self-energy term of the Coulomb energy, denoted by $E_c^{s'}$, is as follows:

$$E_c^{s'} = -\frac{a_c}{A^{1/3}} \left[(Z - k') + k' \frac{R_1}{R_2} \right] = -\frac{a_c}{A^{1/3}} (Z - \varepsilon k'). \quad (\text{B4})$$

This yields Eq. (21).

APPENDIX C: DERIVATION OF $E_c^{e'}$

We begin with the Fermi gas model in which the wave function of a proton is given by

$$\psi(\vec{r}) = \frac{1}{a^{3/2}} e^{i\vec{k}\cdot\vec{r}}, \quad (\text{C1})$$

where a is the length of the box in which a proton is confined, and $\vec{k} = k_x \vec{e}_x + k_y \vec{e}_y + k_z \vec{e}_z$ is its wave vector. The boundary condition yields

$$k_x = \frac{2\pi}{a} n_x, \quad k_y = \frac{2\pi}{a} n_y, \quad k_z = \frac{2\pi}{a} n_z, \quad (\text{C2})$$

where n_x , n_y , and n_z are positive integers. The two-body density operator $\hat{\rho}(\vec{r}, \vec{r}')$ is defined by

$$\hat{\rho}(\vec{r}, \vec{r}') = \sum_{ij} \delta(\vec{r} - \vec{r}_i) \delta(\vec{r}' - \vec{r}_j). \quad (\text{C3})$$

The matrix element of the $\hat{\rho}(\vec{r}, \vec{r}')$ operator is given by

$$\begin{aligned} \rho(\vec{r}, \vec{r}') &= \int \langle \Phi^*(\vec{r}_1, \dots, \vec{r}_Z) | \rho(\vec{r}, \vec{r}') | \Phi(\vec{r}_1, \dots, \vec{r}_Z) \rangle d\vec{r}_1 \dots d\vec{r}_Z \\ &= \rho(\vec{r}) \rho(\vec{r}') - \sum_{ij} \psi_i^*(\vec{r}) \psi_j(\vec{r}) \psi_j^*(\vec{r}') \psi_i(\vec{r}'), \end{aligned} \quad (\text{C4})$$

the first term corresponds to the direct Coulomb energy, and the second term [denoted by $\rho^e(\vec{r}, \vec{r}')$] corresponds to the exchange Coulomb energy on which we focus below. We have

$$\begin{aligned} \rho^e(\vec{r}, \vec{r}') &= \sum_{ij} \psi_i^*(\vec{r}) \psi_j(\vec{r}) \psi_j^*(\vec{r}') \psi_i(\vec{r}') \\ &= \frac{2}{a^6} \sum_{ij} e^{i\vec{k}_i \cdot (\vec{r}' - \vec{r})} e^{i\vec{k}_j \cdot (\vec{r} - \vec{r}')} \\ &= \frac{2}{(2\pi)^6} \int_0^{k_{F1}} e^{i\vec{k}_i \cdot (\vec{r}' - \vec{r})} d\vec{k}_i \int_0^{k_{F1}} e^{i\vec{k}_j \cdot (\vec{r} - \vec{r}')} d\vec{k}_j, \end{aligned} \quad (\text{C5})$$

where k_F is the Fermi momentum of the nuclei. We assume that charge density $\rho = Z/a^3 = k_F^3/(3\pi^2)$ and $x = k_F |\vec{r} - \vec{r}'|$,

and have

$$\int_0^{k_F} e^{i\vec{k} \cdot (\vec{r}' - \vec{r})} d\vec{k} = 4\pi k_F^3 \frac{\sin x - x \cos x}{x^3}.$$

By using this result, Eq. (C5) is reduced to

$$\rho^e(\vec{r}, \vec{r}') = \frac{9}{2} \rho_i \rho_j f(x_i) f(x_j), \quad (\text{C6})$$

where

$$\begin{aligned} x_i &= k_{F1} |\vec{r} - \vec{r}'|, \\ x_j &= k_{Fj} |\vec{r} - \vec{r}'|, \\ f(x) &= \frac{\sin x - x \cos x}{x^3}. \end{aligned}$$

For both the i th and j th protons are in the core part, the exchange term of nuclear Coulomb energy is

$$\begin{aligned} E_{c_1}^{e'} &= -\frac{e^2}{8\pi\epsilon_0} \int \frac{\rho^e(\vec{r}, \vec{r}')}{|\vec{r} - \vec{r}'|} d\vec{r} d\vec{r}' \\ &= -\frac{e^2}{8\pi\epsilon_0} \int \frac{9}{2} \rho_1^2 f^2(x_1) \frac{d\vec{r} d\vec{r}'}{|\vec{r} - \vec{r}'|} \\ &= -\frac{5}{4} \left(\frac{3}{2\pi} \right)^{\frac{2}{3}} \frac{a_c}{A^{1/3}} (Z - k')^{4/3}, \end{aligned} \quad (\text{C7})$$

where $\rho_1 = k_{F1}^3/(3\pi^2)$ is the proton number density in the core part, k_{F1} is the corresponding Fermi momentum, and $x_1 = k_{F1} |\vec{r} - \vec{r}'|$, with $0 \leq x_1 \leq 2k_{F1}R_1$, and k' is the proton number outside the core part. In the last step of the above result, we have made use of the following integral:

$$\int_0^\infty x_1 f^2(x_1) dx_1 = \frac{1}{4}.$$

For cases with both i th and the j th protons are outside the core part, the corresponding exchange term of the Coulomb energy is given by

$$\begin{aligned} E_{c_2}^{e'} &= -\frac{e^2}{8\pi\epsilon_0} \int \frac{9}{2} \rho_2^2 f^2(x_2) \frac{d\vec{r} d\vec{r}'}{|\vec{r} - \vec{r}'|} \\ &= -\frac{5}{4} \left(\frac{3}{2\pi} \right)^{\frac{2}{3}} \frac{a_c k'^{4/3} R_1}{A^{1/3} R_2}, \end{aligned} \quad (\text{C8})$$

where $\rho_2 = k_{F2}^3/(3\pi^2)$ is the proton number density outside the core part with k_{F2} the corresponding Fermi momentum.

For only one of i th and j th protons is inside the core part, the exchange term of the Coulomb energy is given by

$$E_{c_3}^{e'} = -\frac{e^2}{8\pi\epsilon_0} \int \frac{9}{2} \rho_1 \rho_2 f(x_1) f(x_2) \frac{d\vec{r} d\vec{r}'}{|\vec{r} - \vec{r}'|}. \quad (\text{C9})$$

We define $\gamma = \left(\frac{k'}{Z - k'} \right)^{1/3} \left(\frac{R_1}{R_2} \right)$, and obtain

$$\begin{aligned} \rho_2 &= \left(\frac{k'}{Z - k'} \right) \left(\frac{R_1}{R_2} \right)^3 \rho_1 = \gamma^3 \rho_1, \\ x_2 &= k_{F2} |\vec{r} - \vec{r}'| = \left(\frac{k'}{Z - k'} \right)^{1/3} \left(\frac{R_1}{R_2} \right) k_{F1} |\vec{r} - \vec{r}'| = \gamma x_1. \end{aligned}$$

Substituting these two results into Eq. (C9), we have

$$\begin{aligned}
 E_{c_3}^{e'} &= -\frac{e^2}{8\pi\epsilon_0} \int \frac{9}{2} \gamma^3 \rho_1^2 f(x_1) f(\gamma x_1) \frac{d\vec{r}d\vec{r}'}{|\vec{r}-\vec{r}'|} \\
 &= -\frac{e^2}{8\pi\epsilon_0} \int \frac{9}{2} \gamma^3 \rho_1^2 f(x_1) f(\gamma x_1) \frac{d\vec{r}_{12}d\vec{R}}{r_{12}} \\
 &= -\frac{e^2}{8\pi\epsilon_0} \frac{9\gamma^3 \rho_1^2}{2} \frac{4\pi}{k_{F1}^2} \int d\vec{R} \int x_1 f(x_1) f(\gamma x_1) dx_1 \\
 &= -\frac{5}{4} \left(\frac{3}{2\pi} \right)^{\frac{2}{3}} \frac{a_c k'}{A^{1/3}} \left(\frac{R_1}{R_2} \right)^3 (Z - k')^{1/3}, \quad (C10)
 \end{aligned}$$

where $r_{12} = |\vec{r} - \vec{r}'|$, and $\vec{R} = (\vec{r}_1 + \vec{r}_2)/2$. In the last step, we have used an interesting fact that the integral $\int_0^\infty x_1 f(x_1) f(\gamma x_1) dx_1 \simeq \frac{1}{4}$ is almost independent of γ , and equals to 1/4 in the range of interest in this paper.

Summing up the results of Eqs. (C7)–(C10), we obtain the total Coulomb energy of the exchange term as

follows:

$$\begin{aligned}
 E_c^{e'} &= -\frac{e^2}{8\pi\epsilon_0} \int \frac{\rho^e(\vec{r}, \vec{r}')}{|\vec{r}-\vec{r}'|} d\vec{r}d\vec{r}' \\
 &= E_{c_1}^e + E_{c_2}^e + E_{c_3}^e \\
 &= -\frac{5}{4} \left(\frac{3}{2\pi} \right)^{\frac{2}{3}} \frac{a_c}{A^{1/3}} \left[(Z - k')^{4/3} + k'^{4/3} \frac{R_1}{R_2} \right. \\
 &\quad \left. + k' \left(\frac{R_1}{R_2} \right)^3 (Z - k')^{1/3} \right]. \quad (C11)
 \end{aligned}$$

The exchange term of the Coulomb energy $E_c^{e'}$ in terms of $\varepsilon = (R_2 - R_1)/R_2$ finally yields

$$\begin{aligned}
 E_c^{e'} &= -\frac{5}{4} \left(\frac{3}{2\pi} \right)^{\frac{2}{3}} \frac{a_c}{A^{1/3}} [(Z - k')^{4/3} + (k')^{4/3} (1 - \varepsilon) \\
 &\quad + k' (1 - \varepsilon)^3 (Z - k')^{1/3}]. \quad (C12)
 \end{aligned}$$

This gives Eq. (22).

-
- [1] D. Lunney, J. M. Pearson, and C. Thibault, *Rev. Mod. Phys.* **75**, 1021 (2003).
- [2] K. Blaum, *Phys. Rep.* **425**, 1 (2006).
- [3] J. Dufflo and A. P. Zuker, *Phys. Rev. C* **52**, R23(R) (1995).
- [4] P. Möller, J. R. Nix, W. D. Myers *et al.*, *At. Data Nucl. Data Tables* **59**, 185 (1995).
- [5] P. Möller, W. D. Myers, H. Sagawa, and S. Yoshida, *Phys. Rev. Lett.* **108**, 052501 (2012).
- [6] S. Goriely, N. Chamel, and J. M. Pearson, *Phys. Rev. Lett.* **102**, 152503 (2009).
- [7] N. Wang, Z. Liang, M. Liu, and X. Wu, *Phys. Rev. C* **82**, 044304 (2010).
- [8] N. Wang, M. Liu, X. Z. Wu *et al.*, *Phys. Lett. B* **734**, 215 (2014).
- [9] G. Audi, A. H. Wapstra, and C. Thibault, *Nucl. Phys. A* **729**, 337 (2003).
- [10] G. Audi, M. Wang, A. H. Wapstra *et al.*, *Chin. Phys. C* **36**, 1287 (2012); M. Wang, G. Audi, A. H. Wapstra *et al.*, *ibid.* **36**, 1603 (2012).
- [11] W. J. Huang, G. Audi, M. Wang *et al.*, *Chin. Phys. C* **41**, 030002 (2017); M. Wang, G. Audi, F. G. Kondev *et al.*, *ibid.* **41**, 030003 (2017).
- [12] G. T. Garvey and I. Kelson, *Phys. Rev. Lett.* **16**, 197 (1966); G. T. Garvey, W. J. Gerace, R. L. Jaffe *et al.*, *Rev. Mod. Phys.* **41**, S1 (1969).
- [13] I. Kelson and G. T. Garvey, *Phys. Lett.* **23**, 689 (1966).
- [14] G. J. Fu, H. Jiang, Y. M. Zhao, S. Pittel, and A. Arima, *Phys. Rev. C* **82**, 034304 (2010); G. J. Fu, Y. Lei, H. Jiang, Y. M. Zhao, B. Sun, and A. Arima, *ibid.* **84**, 034311 (2011).
- [15] H. Jiang, G. J. Fu, B. Sun, M. Liu, N. Wang, M. Wang, Y. G. Ma, C. J. Lin, Y. M. Zhao, Y. H. Zhang, Z. Ren, and A. Arima, *Phys. Rev. C* **85**, 054303 (2012).
- [16] J. Jänecke, *Phys. Rev. C* **6**, 467 (1972).
- [17] J. Tian, N. Wang, C. Li, and J. Li, *Phys. Rev. C* **87**, 014313 (2013).
- [18] Y. Y. Zong, M. Q. Lin, M. Bao, Y. M. Zhao, and A. Arima, *Phys. Rev. C* **100**, 054315 (2019).
- [19] Y. Y. Zong, C. Ma, Y. M. Zhao, and A. Arima, *Phys. Rev. C* **102**, 024302 (2020).
- [20] C. Ma, Y. Y. Zong, Y. M. Zhao, and A. Arima, *Phys. Rev. C* **102**, 024330 (2020).
- [21] M. Bao, Y. Lu, Y. M. Zhao, and A. Arima, *Phys. Rev. C* **94**, 044323 (2016).
- [22] B. C. Carlson and I. Talmi, *Phys. Rev.* **96**, 436 (1954).
- [23] S. Sengupta, *Nucl. Phys.* **21**, 542 (1960).
- [24] J. A. Nolen and J. P. Schiffer, *Annu. Rev. Nucl. Sci.* **19**, 471 (1969).
- [25] M. Wang, W. J. Huang, F. G. Kondev *et al.*, *Chin. Phys. C* **45**, 030003 (2021).
- [26] K. Blaum, J. Dilling, and W. Nörtershäuser, *Phys. Scr.* **T152**, 014017 (2013).
- [27] C. Y. Fu, Y. H. Zhang, M. Wang, X. H. Zhou, Y. A. Litvinov, K. Blaum, H. S. Xu, X. Xu, P. Shuai, Y. H. Lam, R. J. Chen, X. L. Yan, X. C. Chen, J. J. He, S. Kubono, M. Z. Sun, X. L. Tu, Y. M. Xing, Q. Zeng, X. Zhou *et al.*, *Phys. Rev. C* **102**, 054311 (2020).
- [28] Y. H. Zhang, P. Zhang, X. H. Zhou, M. Wang, Y. A. Litvinov, H. S. Xu, X. Xu, P. Shuai, Y. H. Lam, R. J. Chen, X. L. Yan, T. Bao, X. C. Chen, H. Chen, C. Y. Fu, J. J. He, S. Kubono, D. W. Liu, R. S. Mao, X. W. Ma *et al.*, *Phys. Rev. C* **98**, 014319 (2018).
- [29] D. Puentes, G. Bollen, M. Brodeur, M. Eibach, K. Gulyuz, A. Hamaker, C. Izzo, S. M. Lenzi, M. MacCormick, M. Redshaw, R. Ringle, R. Sandler, S. Schwarz, P. Schury, N. A. Smirnova, J. Surbrook, A. A. Valverde, A. C. C. Villari, and I. T. Yandow, *Phys. Rev. C* **101**, 064309 (2020).
- [30] L. J. Sun, X. X. Xu, S. Q. Hou *et al.*, *Phys. Lett. B* **802**, 135213 (2020).
- [31] See Supplemental Material at <http://link.aps.org/supplemental/10.1103/PhysRevC.105.034321> for predicted mass excesses of 162 proton-rich nuclear masses which are experimentally unaccessible in the AME2020 database, for mass number $14 \leq A \leq 99$.